PERGAMON

Micron 32 (2001) 851–856

micron

www.elsevier.com/locate/micron

Effects of microalloying with Cd and Ag on the precipitation process of Al–4Cu–0.3Mg (wt%) alloy at 200°C

Bondan T. Sofyan[a], K. Raviprasad[a], Simon P. Ringer[b,*]

[a]*Department of Materials Engineering, Monash University, Victoria 3800, Australia*
[b]*Electron Microscope Unit, Madsen Bldg F09, University of Sydney, NSW 2006, Australia*

Abstract

The present work investigates the effects of individual and combined additions of Cd and Ag on precipitation processes in an Al–4Cu–0.3Mg (wt%) alloy. Analytical scanning transmission electron microscopy revealed that microalloying with Cd stimulates nucleation of θ' phase on $\{001\}_\alpha$ planes and that Cd-rich particles form on the rim and broad facets of the θ' platelets. We interpret these observations to suggest that Cd nucleates heterogeneously at the θ'–α interface and that θ' can also nucleate heterogeneously at the Cd–α interface. In the quinary alloy, it was observed that Ag and Cd additions seem to work independently resulting in a fine and uniform dispersion of both Ω and θ'. Furthermore, the hardening effect of the $\{111\}_\alpha$ Ω phase appears to be more potent than other precipitates formed in this system since the hardness of the quinary alloy was intermediate between the Al–Cu–Mg–Ag and the Al–Cu–Cd alloys. © 2001 Elsevier Science Ltd. All rights reserved.

Keywords: Al–Cu–Mg alloys; Cd addition; Ag addition; θ' phase; Ω phase; σ phase; Cu–Mg co-cluster; Mg–Ag co-cluster

1. Introduction

It is well known that trace or microalloying additions to Al alloys can strongly influence the precipitation phenomena and this has great practice importance (Polmear and Ringer, 2000). These additions can modify the dispersion and/or the habit plane, morphology and crystal structure of the resulting precipitation. For example, Al–Cu alloys microalloyed with Cd, Sn or In are known to possess a finer and more uniform dispersion of θ' on the $\{001\}_\alpha$ planes and exhibit an increased hardening response (Silcock et al., 1955–1956). Various mechanisms have been proposed for this effect, although recent one-dimensional atom probe (1DAP) experiments on an Al–Cu–Sn alloy have shown that Sn atoms cluster rapidly during or immediately following the quench from solution treatment and that this is followed by precipitation of pure β-Sn and θ' (Al_2Cu) such that the Sn is associated with the partially coherent rim of θ' platelets (Ringer et al., 1995a). Kanno et al. (1980) have observed In-rich precipitates in Al–Cu–In alloys and Taylor et al. (1978) have reported a refined dispersion of θ' and enhanced hardening in Al–Cu–Mg–Cd alloys. Microalloying with Cd has the advantage that, unlike Sn and In, it does not form an intermetallic compound with Mg.

On the other hand, trace additions of Mg and, in particular, Mg and Ag to Al–Cu alloys promote precipitation of Al_2Cu on $\{111\}_\alpha$ designated Ω (Polmear and Chester, 1989; Garg and Howe, 1991). Although Ω forms as only a minor phase in ternary Al–Cu–Mg alloys, it forms in very high number densities ($\sim$2192 μm^{-3}) in quaternary Al–Cu–Mg–Ag alloys and this precipitate dispersion is associated with significant strengthening (Ringer et al., 1995b; Polmear and Couper, 1988). Using 1DAP, it was shown recently that Mg–Cu co-clusters predominate during the early stages of ageing in ternary Al–Cu–Mg alloys and that Ag additions result in a predominance of Mg–Ag co-clusters (Ringer et al., 1996). Initially, these Mg–Ag co-clusters possess a complex undefined shape. Eventually, as more solute accumulates in the clusters, they develop a more compact disc-like shape on $\{111\}_\alpha$ planes and these features seem to nucleate the $\{111\}_\alpha$ Ω phase (Reich et al., 1998).

This work is a summary of observations of the effect of individual and combined additions of Cd and Ag to a ternary Al–4Cu–0.3Mg (wt%) alloy. In particular, analytical transmission electron microscopy (ATEM) was used to examine whether precipitation of both θ' and Ω could be stimulated in the same alloy.

2. Experimental

Four alloys were used in this study and their compositions

* Corresponding author.

0968–4328/01/$ - see front matter © 2001 Elsevier Science Ltd. All rights reserved.
PII: S0968-4328(00)00093-7

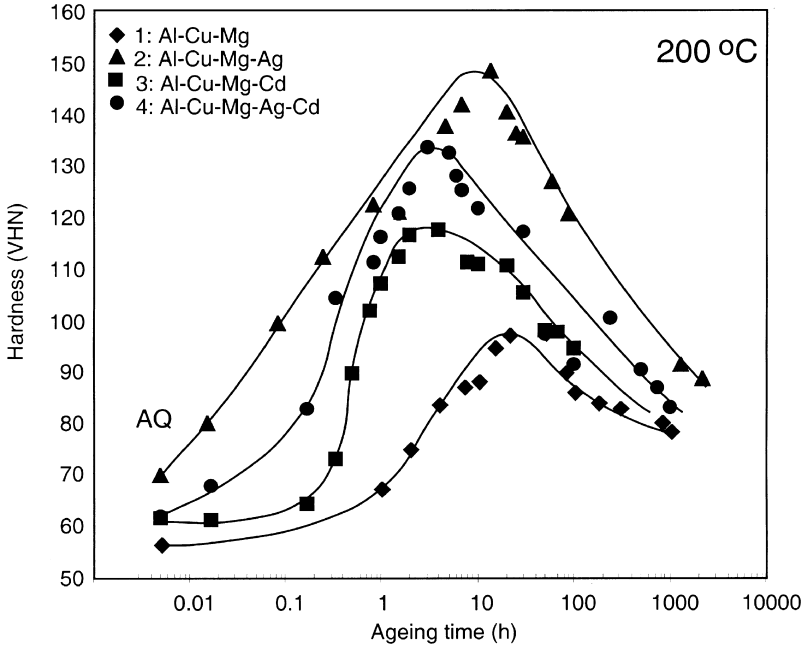

Fig. 1. Age hardening curves at 200°C. AQ: as quenched.

are provided in Table 1. Samples of each were solution treated at 525°C for 1 h and then quenched into cold water. Ageing was conducted at 200°C and the hardening response monitored by Vickers hardness measurements under a 5 kg load. The evolution of microstructure was followed using a Philips CM20 analytical scanning transmission electron microscope (ASTEM) operating at 200 kV equipped with an Oxford Instruments LINK energy dispersive X-ray spectrometer (EDXS). Samples for ASTEM were prepared in a twin jet polisher using a solution of 1 : 2 vol.% nitric acid:methanol at −25°C. Qualitative EDXS was performed in STEM nanoprobe mode with a probe size of nominal diameter ∼5 nm and the electron beam parallel to the $\langle 001 \rangle_\alpha$ zone axis. Careful tilting was conducted to ensure that the electron scattering arose principally from the probed phase, with minimal contributions from the matrix.

3. Results and discussion

3.1. Age hardening response

Fig.1 indicates that all alloys exhibit single stage age hardening at 200°C; however, alloys 1 and 3 also have an incubation period of 1 h and ∼10 min, respectively.

Table 1
Nominal and (actual) composition of alloys studied in wt%

Alloy	Cu	Mg	Ag	Cd	Al
Alloy 1	4 (3.35)	0.3 (0.27)	–	–	Balance
Alloy 2	4 (4.30)	0.3 (0.28)	0.4 (0.38)	–	Balance
Alloy 3	4 (4.38)	0.3 (0.26)	–	0.5 (0.54)	Balance
Alloy 4	4 (4.73)	0.3 (0.20)	0.4 (0.55)	0.5 (0.41)	Balance

Confirming previous results (Taylor et al., 1978), the addition of Cd to the ternary Al–Cu–Mg alloy increases the peak hardness significantly. Moreover, we note that the Al–Cu–Mg–Ag alloy possesses the highest hardness and that the quinary Al–Cu–Mg–Ag–Cd alloy possesses an intermediate peak hardness.

3.2. Precipitation processes

As the base alloy has a high Cu:Mg ratio, it is expected that the precipitation processes involve those observed in binary Al–Cu alloys (e.g. GP zones $\rightarrow \theta'' \rightarrow \theta' \rightarrow \theta$ (Al_2Cu)) and those observed in the pseudo Al–S alloys (e.g. GPB zone $\rightarrow$ S (Al_2CuMg)). However, no GP zones were expected to form during ageing at 200°C, as this is above the GP zone solvus temperature (Beton and Rollason, 1957–1958). The initial incubation period of alloy 1 (Fig. 1) was due to the gradual formation of GPB zones, as has been observed previously (Silcock, 1960–1961). These precipitates were less numerous in alloy 3, where the presence of Cd promotes the precipitation of θ' phase and gives rise to an accelerated ageing response. Alloys 2 and 4 commence the hardening at the outset of ageing.

Bright field (BF) TEM images of the peak hardness microstructure for each alloy during ageing at 200°C were recorded close to the $\langle 001 \rangle_\alpha$ zone axis and examples are provided in Fig. 2. The description of these peak hardness microstructures is summarized in Table 2. Lath-shaped S phase precipitates having a $\{210\}_\alpha$ habit plane together with θ' dominated the microstructure of alloy 1 (Fig. 2(a)). The corresponding SAED pattern shows reflections and streaks along $\langle 001 \rangle_\alpha$ directions through the $\{011\}_\alpha$ position together with sharp streaks through the $\{020\}_\alpha$ reflections along the $\langle 001 \rangle_\alpha$

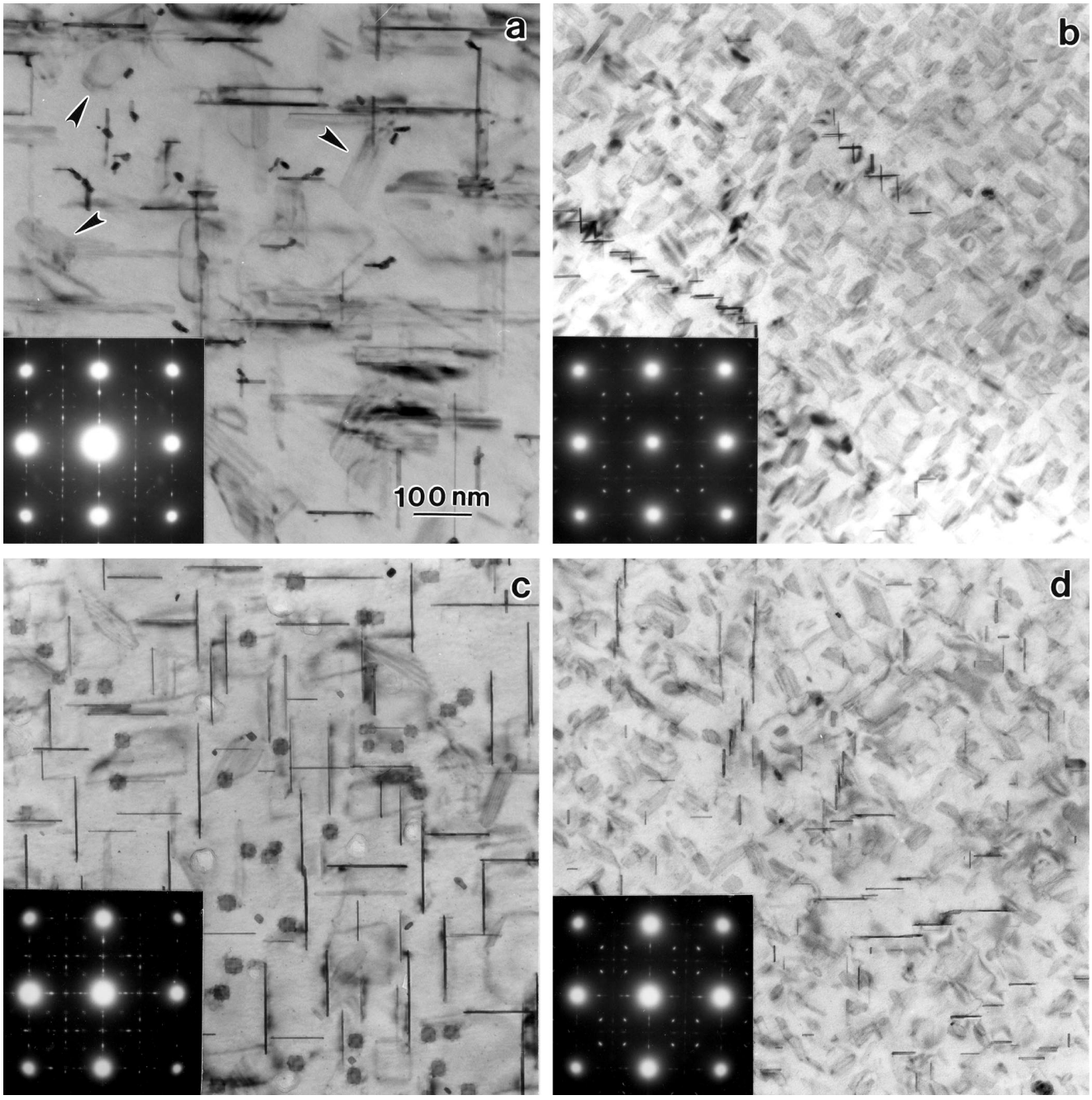

Fig. 2. $\langle 001 \rangle_\alpha$ TEM BF micrographs and corresponding SAED patterns of (a) Al–Cu–Mg, (b) Al–Cu–Mg–Ag, (c) Al–Cu–Mg–Cd and (d) Al–Cu–Mg–Ag–Cd alloys aged to peak hardness at 200°C. Scale bar applies to all micrographs.

direction which are consistent with the S and θ' phase, respectively. In addition, the Ω phase was also observed to precipitate on $\{111\}_\alpha$ planes (arrowed), although the low number density of these precipitates meant that the characteristic shape effects were difficult to observe.

As already extensively studied before, the addition of Ag to Al–Cu–Mg alloy (alloy 2) stimulates precipitation of the Ω phase on $\{111\}_\alpha$ plane. These precipitates are inclined to the $\langle 001 \rangle_\alpha$ beam direction in Fig. 2(b). It is clear that the dispersion of Ω phase is very fine and uniform, as confirmed by the strong reflections on 1/3 and 2/3 $\mathbf{g}\{220\}_\alpha$ in the SAED (selected area electron diffraction) pattern. In addition, arrays of θ' precipitates heterogeneously nucleated on dislocations were also observed; however, no S phase was observed. The presence of Ω phase on $\{111\}_\alpha$ plane in this alloy resulted in the highest age hardening response (Fig. 1).

The microstructure of alloy 3 at peak hardness contains a uniform dispersion of θ' (Fig. 2(c)). The number density of θ' in this alloy was obviously higher than that observed in the other alloys. This confirms the proposal made by Taylor et al. (1978) that the enhanced hardening associated with Cd additions is due to the promotion of the θ' phase. Moreover,

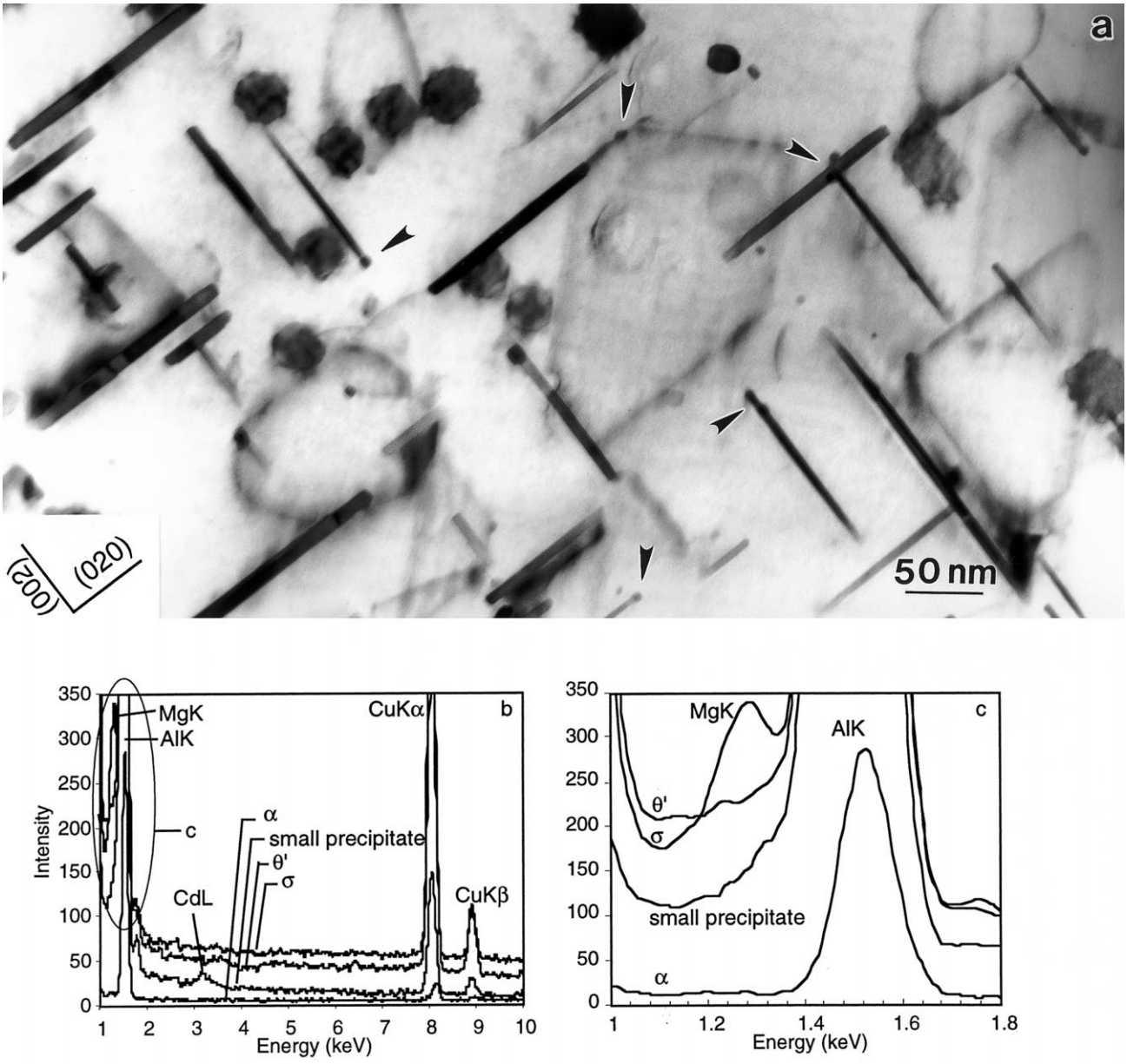

Fig. 3. (a) $\langle 001 \rangle_\alpha$ TEM BF micrograph of Al–Cu–Mg–Cd alloy aged at 200°C for 200 h showing small precipitates on the rim and broad facets of θ' plates. (b) and (c) Typical EDXS spectra of the matrix, small precipitate, θ' and σ phase.

the present results suggest that the action of Cd in ternary Al–Cu–Mg alloys is effectively the same as that proposed to occur in binary Al–Cu. The presence of numerous small precipitates at diameter ~2–4 nm were observed as the first precipitate and these persisted throughout the ageing process. In the overaged sample, it was clear that these small precipitates were associated with both the partially-coherent rim-facet and the broad-facets of the θ' platelets (arrowed, Fig. 3(a)).

The cuboidal σ phase ($Al_5Cu_6Mg_2$) exhibits a simple orientation relationship with α-Al: $\langle 100 \rangle_\alpha // \langle 100 \rangle_\alpha$ and $\{100\}_\alpha // \{100\}_\alpha$. This phase has been observed mainly in Si-containing Al–Cu–Mg alloys (Schueller et al., 1994), and more recently in Al–Cu–Mg–Ag alloys (Li and Wawner, 1997). These precipitates were observed uniformly throughout the peak hardness and overaged microstructures. It is proposed that the stimulation of θ' precipitates by Cd leaves an excess of Mg in the matrix so that precipitation of the σ phase is promoted.

The peak hardness microstructure of alloy 4 indicates that combined additions of Ag and Cd promote separately the precipitation of Ω phase on $\{111\}_\alpha$ planes and θ' on $\{001\}_\alpha$ planes in a fine and uniform dispersion, Fig. 2(d). The composite microstructure of θ' and Ω precipitates on their respective habit planes indicates that these phases may be stimulated individually or in combination, by selected microalloying. Qualitative estimation of the number density of θ' and Ω precipitates in alloy 4 suggested that, in each

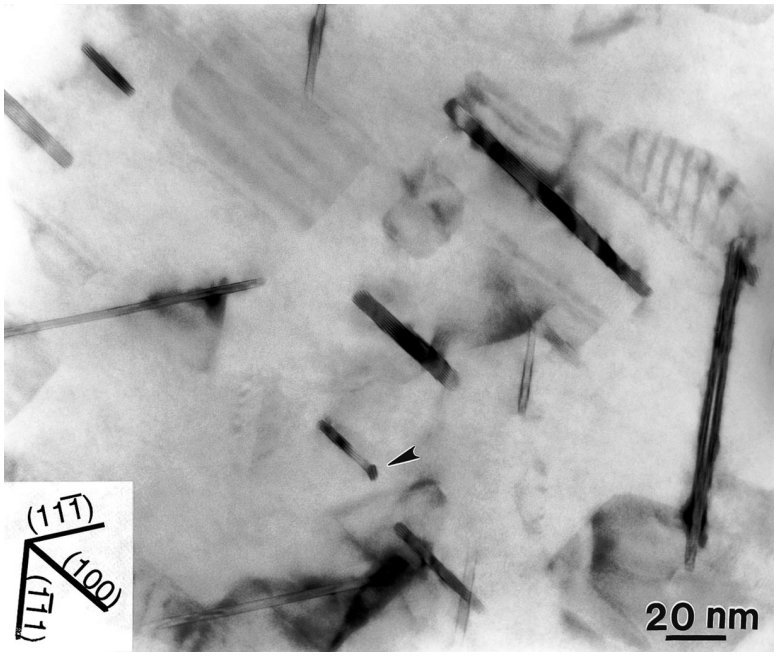

Fig. 4. $\langle 110 \rangle_\alpha$ TEM BF image of Al–Cu–Mg–Ag–Cd alloy aged at 200°C for 200 h showing small Cd-rich precipitate on the rim of θ' platelets.

case, they were intermediate between those observed in the quaternary alloys 2 and 3. This seems consistent with the measured hardness response, where the peak hardness of alloy 4 is intermediate between alloys 2 and 3. Fig. 2(d) also reveals numerous small (~2–4 nm in diameter) precipitates. These are more clearly observed after coarsening associated with overageing, Fig. 4. Microanalysis using STEM–EDXS revealed that they are also Cd-rich particles, as found for alloy 3.

The composition of precipitates in the overaged microstructure was assessed using STEM–EDXS so as to infer details of the microstructural evolution. X-ray spectra were acquired with the electron beam parallel to the $\langle 001 \rangle_\alpha$ zone axis. Typical X-ray spectra from the matrix, small precipitates, θ' and the σ phase are provided in Fig. 3(b). No Cd was detected in the matrix and this is consistent with predictions from the Al–Cd phase diagram, which indicate that Cd is immiscible in Al (Massalski, 1990). However, a clear Cd signal was detected from analyses of the small precipitates in contact with θ'. The Cu peak also observed in these analyses is likely to arise from the adjacent θ' (Al_2Cu). This provides direct support for the proposal by Sankaran and Laird (1974) that the precipitates observed at the edges and corners of θ' platelets in Cd-bearing Al–Cu alloys are Cd-rich particles. Those authors proposed that the Cd precipitates reduce the interfacial energy and the lattice mismatch along the c direction for the θ'–α interface and hence stimulate θ' phase precipitation by providing good matching. However, we would suggest that the presence of Cd-rich precipitates in contact with θ' arises from a preferred nucleation of θ' at Cd precipitates (and also vice versa), and that the effect is similar in origin to the way that Sn and In nucleate θ' in Al–Cu–Sn/In (Ringer et al., 1995a; Kanno et al., 1980).

Table 2
Summary of peak hardness microstructure following ageing at 200°C

Alloy	Qualitative description of precipitation observed in the peak hardness microstructure
Al–Cu–Mg	Large S (Al_2CuMg) laths in a uniform distribution Coarse dispersion of θ' (Al_2Cu) Occasional Ω (Al_2Cu) platelets
Al–Cu–Mg–Ag	Fine and uniform dispersion of Ω phase Arrays of θ' phase on quenched-in defects
Al–Cu–Mg–Cd	Fine and uniform dispersion of θ' phase Uniform distribution of σ ($Al_5Cu_6Mg_2$) phase Occasional S phase precipitates Rare Ω phase precipitates
Al–Cu–Mg–Ag–Cd	Fine and uniform dispersion of Ω precipitates Fine and uniform dispersion of θ' precipitates

The observations on the effect of Cd and Ag on the precipitation and hardening in Al–4Cu–0.3Mg (wt%) provide some insights into the relative interactions between alloying elements. It is generally accepted that the co-clustering of Cu and Mg in ternary Al–Cu–Mg alloys leads to the precipitation of GPB zones and S phase, while the co-clustering of Mg and Ag in quaternary Al–Cu–Mg–Ag alloys leads to the nucleation of Ω phase (Ringer et al., 1996; Reich et al., 1998). The enhancement of Ω and the absence of S phase at peak hardness in alloy 2 (Fig. 2(a) and (b)) suggest that the Mg–Ag interaction predominates over the Mg–Cu interaction and this is further supported by the observation that no σ phase was observed in alloy 4 at peak hardness, while this phase precipitated extensively in alloy 3. It is thought that most of the available Mg atoms are attracted to Ag and vacancies and participate in the nucleation of the Ω phase,

leaving insufficient residual Mg in the matrix to form σ phase.

In alloy 2, it is also interesting to note that the θ' platelets were observed in a non-uniform distribution, typical of heterogeneous nucleation on dislocations (Fig. 2(b)), together with a uniform distribution of Ω phase. This supports the above suggestion that the precipitation of θ' on $\{001\}_\alpha$ and of Ω phase on $\{111\}_\alpha$ are effectively independent processes and this proposal seems to be verified by the observations in alloy 4 that the combined effects of Mg and Cd gave rise to the enhanced nucleation of both Ω and θ' phases, Fig. 2(d).

4. Conclusions

1. Combined additions of Cd and Ag promote the precipitation of both θ' phase on $\{100\}_\alpha$ planes and Ω phase on $\{111\}_\alpha$ planes. This suggests that the interaction between the formation of Cd-rich precipitates and θ' nucleation is effectively independent of the co-clustering of Mg–Ag atoms and subsequent nucleation of Ω phase.
2. In Al–Cu–Mg–Cd and Al–Cu–Mg–Ag–Cd alloys, θ' precipitation occurs in a fine and uniform dispersion after ~30 min at 200°C.
3. Microanalysis using STEM–EDXS revealed that nanoscale Cd-rich precipitates form in Al–Cu–Mg–Cd and Al–Cu–Mg–Ag–Cd alloys. These precipitates are associated with both the partially coherent rim-facets and the coherent broad-facets of the θ' platelets.

Acknowledgements

The authors acknowledge gratefully helpful discussions with Emeritus Professor I.J. Polmear of the Department of Materials Engineering, Monash University. BTS acknowledges financial support from the Australian Agency for International Development. RK is supported by Monash University's Logan Research Fellow Scheme.

References

Beton, R.J., Rollason, E.C., 1957–1958. Hardness reversion of dilute aluminium–copper and aluminium–copper–magnesium alloys . J. Inst. Met. 86, 77.

Garg, A., Howe, A.M., 1991. Nucleation and growth of Ω phase in Al–4.0Cu–0.5Mg–0.5Ag alloy—an in situ hot-stage TEM study. Acta Met. Mater. 39 (8), 1925.

Kanno, M., Suzuki, H., Kanoh, O., 1980. The precipitation of θ' phase in an Al–4%–Cu–0.06%In alloy. J. Japan Inst. Light Met. 44, 1139.

Li, Q., Wawner, F.E., 1997. Characterization of a cubic phase in an Al–Cu–Mg–Ag alloy. J. Mater. Sci. 32, 5363.

Massalski, T.B., 1990. Binary Alloy Phase Diagram. . 2nd ed.ASM, Ohio.

Polmear, I.J., Chester, R.J., 1989. Abnormal age hardening in an Al–Cu–Mg alloy containing silver and lithium. Scripta Met. 23, 1213.

Polmear, I.J., Couper, M.J., 1988. Design and development of an experimental wrought aluminium alloy for use at elevated temperature. Met. Trans. A 19A, 1027.

Polmear, I.J., Ringer, S.P., 2000. Advanced aluminium alloy design. J. Japan Inst. Light Metal 50, 633–642.

Reich, L., Murayama, M., Hono, K., 1998. Evolution of Ω phase in Al–Cu–Mg–Ag alloy—a three-dimensional atom probe study. Acta Mater. 46 (17), 6053.

Ringer, S.P., Hono, K., Polmear, I.J., Sakurai, T., 1996. Nucleation of precipitates in aged Al–Cu–Mg– (Ag) alloys with high Cu:Mg ratios. Acta Mater. 44 (5), 1883.

Ringer, S.P., Hono, K., Sakurai, T., 1995a. The effect of trace addition of Sn on precipitation in Al–Cu alloys: an atom probe ion microscopy study. Met. Mater. Trans. A 26A, 2207.

Ringer, S.P., Muddle, B.C., Polmear, I.J., 1995b. Effects of cold work on precipitation in Al–Cu–Mg– (Ag) and Al–Cu–Li– (Mg–Ag) alloys. Met. Mater. Trans. A 26A, 1659.

Sankaran, R., Laird, C., 1974. Effects of trace additions Cd, In and Sn on the interfacial structure and kinetics of growth of θ' plates in Al–Cu alloy. Mater. Sci. Eng. 14, 271.

Schueller, R.D., Wawner, F.E., Sachdev, A.K., 1994. Nucleation mechanism of the cubic σ phase in Squeeze-Cast Aluminium Matrix Composites. J. Mater. Sci. 29, 424.

Silcock, J.M., Heal, T.J., Hardy, H.K., 1955–1956. The structural ageing characteristics of ternary aluminium–copper alloys with cadmium, indium or tin. J. Inst. Met. 84, 23.

Silcock, J.M., Heal, T.J., Hardy, H.K., 1960–1961. The structural ageing characteristics of Al–Cu–Mg alloys with copper:magnesium weight ratios of 7:1 and 2.2:1. J. Inst. Met. 89, 203.

Taylor, J.A., Parker, B.A., Polmear, I.J., 1978. Precipitation in Al–Cu–Mg–Ag casting alloy. Metal Sci. October, 478.